Int. J. Heat Mass Transfer. Vol. 21, pp. 769–781

0017-9310/78/0601-0769 $02.00/0

HIGH TEMPERATURE GAS DIAGNOSTICS BY SPECTRAL REMOTE SENSING

P. J. HOMMERT* and R. VISKANTA
Heat Transfer Laboratory, School of Mechanical Engineering, Purdue University, West Lafayette, IN, U.S.A.

(*Received* 28 *April* 1977 *and in revised form* 5 *October* 1977)

Abstract—The usefulness of spectral emission measurements in determining line-of-sight temperature and/or concentration distributions in high temperature gaseous systems is investigated. An analytical model was constructed which relates the emitted spectral intensity to the local temperature and radiating species concentration within the gas. The mathematical statement of the model leads to a series of integral equations, one for each frequency at which data are taken. The profiles within the gas are determined by inverting these integral equations through the use of a parameter estimation inversion technique. In addition to a series of analytical experiments, experimental verification study was conducted in which gas temperatures varying from 700 to 1350 K over a 25 cm path were produced in an electrically heated furnace. The gas consisted of CO_2/N_2 mixtures whose relative mole fractions could be varied with the total pressure remaining constant at 1 atm. Temperature profiles determined by inversion agreed with profiles based on a combination of predictions and independent thermocouple measurements with an average error of less than 3% (using the independently measured CO_2 partial pressure).

NOMENCLATURE

- f, function defined by equation (5);
- I_ν, spectral intensity of radiation;
- $I_{b\nu}$, Planck's function;
- k, mass absorption coefficient;
- L, system length;
- s, spatial coordinate;
- T, temperature;
- X, optical thickness defined by equation (7).

Greek symbols

- α, solution parameters;
- κ, volumetric absorption coefficient;
- ν, frequency;
- ξ, nondimensional length coordinate s/L;
- ρ, density of reflectance;
- τ, transmittance.

Subscripts

- B, background;
- b, blackbody;
- ν, frequency.

INTRODUCTION

IN RECENT years optical techniques for the measurement of temperature have become increasingly popular. The application of one such technique, spectral remote sensing (or spectral scanning), for determining line of sight gas temperature profiles is the subject of this paper.

Spectral scanning involves the measurement with some appropriate sensor of the spectral distribution of natural emission (usually infrared) from the system under study. The spectral radiation field emerging from the system is the result of emission and reabsorption of radiation by the medium. Each volume element along the line of sight contributes to this emission. Locally, of course, the volumetric emission coefficient [1] depends on the spectral absorption coefficient of the medium and the local temperature. Along a given path, the entire medium contributes in varying proportion to the measured emitted (emerging) intensity. In addition, the spatial variation of the contributions is frequency dependent. This makes the spectral intensity emerging from the medium a function of the temperature and concentration distributions within the radiating species, and makes it possible to identify the system on the basis of observations of its output. Specifically, a so-called inversion procedure is used to obtain from the set of integral equations describing the measured spectral emission information about the distribution of temperature and concentration within the radiating species.

The advantages of such an approach in combustion systems are: (1) it is noninterfering since it does not require probes; (2) it is passive in that there is no need for an external source of electromagnetic radiation; (3) the measurements can be made from remote locations provided the effect, if any, of the intervening medium is accounted for; and (4) relatively simple instrumentation is required for emission measurements. The limitations result primarily from: (1) the need for the presence of a strong I.R. emitter and for (2) a finite number of independent data points, (3) effects of concentration variations, and (4) errors introduced by inaccuracies in modeling the spectral absorption characteristics of the radiating species and approximations needed to predict nonhomogeneous gas emission.

*Presently at Sandia Laboratories, Albuquerque, NM, U.S.A.

Spectral scanning has become an accepted technique for atmospheric sounding problems where it is desired to determine temperature and concentration profiles in the atmosphere from satellite measurements [2].

For high temperature gases, the emphasis of this paper, there have been relatively few applications [3–7]. Most notable among these is the work of Cutting [6] and Cutting and McStewart [7]. In addition to a detailed comparison of the iterative inversion procedure, they conducted experimental studies in a tube furnace. The iterative procedure employed did not require simple profile shapes or restrict the number of zones in which the temperature could be determined. Using spectral emission measurements in the 4.3 μm band, temperature profiles are determined within 5% of the measured. Beyond the peak the temperatures determined are not as accurate, for reasons that will be discussed later in this study. A double-sided inversion procedure is suggested to overcome this; however, conditions did not allow for it to be studied experimentally. Although the effects of concentration variations are discussed, the determination of concentration profiles is not explicitly investigated.

A number of aspects of spectral remote sensing as applied to high temperature gases that have not been examined by other studies [3–7] are treated in this work. These include: (1) attempting to determine the emitting species concentration in addition to the temperature profile; (2) investigating the effect of a high emittance rear boundary; (3) investigating the use of an optimization routine in the parameter estimation approach to spectral inversion; and (4) demonstrating the use of a low spectral resolution instrument as opposed to the spectrometers typically used.

ANALYTICAL STUDY

Physical model and basic equations

Figure 1 shows a schematic diagram of the basic physical situation and coordinate system for the analysis. A mass of gas containing an infrared absorbing emitting species with a temperature gradient and potentially a concentration gradient is considered. The physical dimension L will be known for an internal system; for an external system it may have to be approximated. There may be a known or measurable radiation intensity incident at the back side of the region $I_\nu(L)$ either from an external source, as in the case of an absorption measurement, or from a high temperature wall boundary. The temperature and concentration are assumed to vary in the s direction.

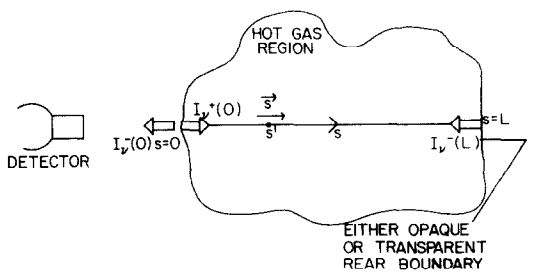

FIG. 1. Physical model and coordinate system.

In order to proceed with the mathematical formulation it is necessary to make two additional assumptions: First, the system is in local thermodynamic equilibrium (LTE) which allows for the use of Kirchoff's and Planck's laws to describe emission and absorption of radiation in the gas, and second, the medium is nonscattering. For the conditions of this study both these assumptions are satisfied.

Radiation transfer in a participating medium is based on a fundamental equation resulting from a radiant energy balance on a pencil of radiation propagating in a given direction s. Under the assumptions mentioned, the spectral intensity $I_\nu(s)$ defining the radiation field is governed by the radiative transfer equation [1] which for a medium of refractive index unity is given as

$$\frac{dI_\nu(s)}{ds} = k(\nu, T)\rho(s)[I_{b\nu}[T(s)] - I_\nu(s)] \quad (1)$$

where $I_{b\nu}[T(s)]$ is Planck's function, $k(\nu, T) = \kappa(\nu, T)/\rho$ is the mass absorption coefficient, and $\rho(s)$ is the local density.

Equation (1) indicates that the spectral intensity $I_\nu(s)$ is increased by emission and decreased by absorption in the path length ds. To analyze the case where the rear boundary is opaque, one can proceed by breaking the radiation field into two components, one directed in the positive direction (superscript +) and the other in the negative direction (superscript −), see Fig. 1. Applying the following conditions

$$I_\nu^-(0) = 0 \quad (2)$$

and

$$I_\nu^-(L) = \rho_B I_\nu^-(L) + \varepsilon_B I_{b\nu}(T_B) \quad (3)$$

equation (1) can be solved in both directions with the results combined to yield the emerging spectral intensity

$$I_\nu^-(0) = \int_0^L I_{b\nu}[T(s')]\left\{-d\tau_\nu(s')/ds'\right. + \rho_B \exp\left[-\left(2\int_0^L \rho(s'')k(\nu, T)\,ds'' - \int_0^{s'} \rho(s'')k(\nu, T)\,ds''\right)\right]\left.ds'\right\} + \varepsilon_B I_{b\nu}(T_B)\tau_\nu(L) \quad (4)$$

where the transmittance τ_ν is defined as

$$\tau_\nu = \exp\left[-\int_0^s k(\nu, T)\rho(s')\,ds'\right].$$

The term involving $\rho_B \exp[\ldots]$ in this equation merely accounts for radiation emitted in the backward direction which emerges from the medium after suffering reflection at the rear boundary. This term is small, especially for the situations of this study.

This then is the basic equation of spectral inversion and is a nonhomogeneous Fredholm integral equation of the first kind. It shows that the measured emerging

intensity $I_\nu^-(0)$ is related to the temperature in the medium through Planck's function and a frequency dependent spatial weighting factor (kernel) which is the derivative of the transmittance. The transmittance contains the dependence of $I_\nu^-(0)$ on the concentration distribution.

As seen from equation (4), in order to predict $I_\nu^-(0)$ it is necessary to know not only the temperature and concentration distributions but also the gas transmittances which must be predicted from a formulation that incorporates both these distributions and appropriate physical data. Unfortunately, the spectral absorption and emission of radiation in a gas cannot be characterized by a single parameter such as in the case of semitransparent solids. Factors relating to line shape, line intensity (strength), and line spacing must all be considered.

The first step in the calculation of gas transmittances is, of course, the selection of an appropriate molecule and an associated band whose emission–absorption will be studied. For both the analytical and experimental portions of this study, the 4.3 μm band of CO_2 was selected for the reasons that it is a strong infrared band with only a small overlap, near 4.7 μm, with a much weaker CO band.

In particular the CO_2 transmittances were calculated using the "Goody model", i.e. randomly located lines with an exponential line strength distribution. The particular band model parameters used were those calculated by Malkmus [8] as tabulated by Ludwig *et al.* [9]. The nonhomogeneous effects caused by temperature and concentration variations along the line of sight were handled by the standard Curtis–Godson approximation [10, 11]. The errors involved in using the Curtis–Godson approximation are discussed by Ludwig *et al.* [9].

Inversion procedure

A number of solution procedures have been used in conjunction with the spectral scanning inversion problem. Probably the nonlinear iterative techniques have seen the widest use [12, 13, 6]. These techniques involve iterating on the temperature at various points throughout the medium based on the information content that a particular spectral measurement has about conditions at that point. Since the spatial weighting functions or kernels determine the information content, they are used directly in the nonlinear techniques.

Another approach is that of parameter estimation. Here the desired profile is represented by a parameter set whose values are then determined, through an optimization procedure, to best fit the measured data [14, 15]. Parameter estimation is flexible because it does not require explicit specification of spatial weighting functions and because most problems can be easily posed in an optimization form. Furthermore, a general view of high temperature applications would seem to indicate that a solution in terms of a small set of parameters may not only be sufficient, it may also be all that is attainable from the measured data.

The first step in any optimization problem is the selection of an index of performance or function to be minimized. Since the inversion problem generally involves a set of n measurements of $I_{\nu_i}^-(0)$ with m unknown parameters ($n > m$), it has the characteristic features of a least squares problem so that a least squares comparison of measured and calculated emission data is selected as the index of performance. Specifically, the function f is minimized where

$$f = \sum_{i=1}^{n} [I_{\nu_i,\text{calc}}(0) - I_{\nu_i,\text{meas}}(0)]^2, \tag{5}$$

n being the number of independent spectral measurements made.

The unknowns determined by the optimization routine are a set of polynomial coefficients which specify the profile through the relationship

$$T(\xi)/T_{\text{ref}} = \sum_{i=1}^{m} \alpha_i L_{i-1}(\xi'') \tag{6}$$

where L_i is the ith Legendre polynomial transformed to the interval 0–1. Also, $\xi = s/L$ and η is a space coordinate transformation variable which increases the flexibility of polynomials in fitting various profiles by expanding or contracting them according to its value. Computational details are given elsewhere [16].

To perform the optimization, a standard Fletcher–Powell–Davidon [17, 18] conjugate gradient technique is used. Solution constraints such as the temperature at a certain point or transmissivity at a particular frequency could be imposed by the addition of a penalty function directly to the index of performance.

Analytical experiments

Once a procedure to predict gas emission and an inversion technique have been selected, analytical experiments can be conducted to study spectral inversion as applied to high temperature gases. The term analytical experiment implies that equation (4) is used to predict a set of spectral emission data for assumed temperature and concentration profiles. These data are then employed as input to the inversion procedure discussed, and the determined concentration and temperature profiles can be directly compared to those assumed.

For the analytical experiments the assumed profiles were taken as approximately those expected for the experimental investigations. In particular, the temperature profile is characterized by temperatures around 500 K at the front boundary to peak values of between 1200 and 1400 K. The total pressure is 1 atm with CO_2 partial pressures ranging from 0.05 to 0.4 atm. The remainder of the gas sample is N_2. There is, of course, no concentration gradient as such, the CO_2 having a constant mixing ratio.

Kernels. To understand the type of information spectral emission measurements can supply under these conditions, one must examine the kernels of equation (4). Once again, the kernel ($d\tau_\nu/ds$) determines the contribution through Planck's function

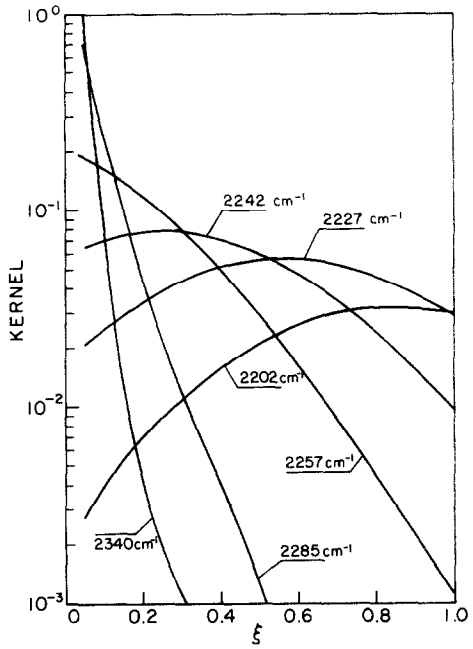

FIG. 2. Kernel ($d\tau/dx$) in equation (4) for typical "furnace" temperature and concentration conditions, $L = 25$ cm.

that the temperature at each point within the gas has in the emitted spectral intensity. Figure 2 shows representative distributions kernel at a number of frequencies for the experimental conditions shown in Figs. 8 and 9. Figure 2 illustrates a number of points. First, the spectral data range is typical of that used to obtain both experimental and analytical results. In particular the P branch of the 4.3 μm CO_2 band between 2350 and 2200 cm^{-1} is used exclusively. For the analytical studies between five and seven data points in this range were employed. The actual number of data points is not critical as long as the full range of optical thicknesses available is covered. The effect of omitting certain optical thicknesses will be discussed in conjunction with experimental results.

With respect to inversion, Fig. 2 indicates that at frequencies near the band center (2340, 2285 cm^{-1}) where the absorption is strong, only the front portion of the gas contributes to the emitted intensity. Thus these points should accurately define a front surface temperature. As frequency is decreased the peak weighting by the kernels shifts further into the gas until at 2202 cm^{-1} the rear side is weighted most heavily. This shift occurs because frequencies away from the band center contribute significantly to the emission only at the higher temperatures. Thus, for these conditions there is a frequency for which each region of the gas that gives a maximum contribution to the emitted spectral intensity. With a kernel distribution such as this an inversion process should be able to determine the temperature accurately throughout the medium.

For analytical experiments the assumed profiles could be fit accurately using only three parameters. Also, the kernels are well structured throughout the path length so that with the use of exact emission data and a specified concentration level, very accurate results would be expected. Indeed, determined and assumed profiles agreed so closely that a graphical comparison is not helpful. Typical test profiles used here are shown in the figures of this subsection. For the entire path length, average temperature errors were in the range of 0.5% with average intensity errors of approximately 1.0%. The results of analytical experiments conducted on more complex profiles are discussed elsewhere [16]. These studies indicated that temperature profiles could be accurately determined by inversion up to the temperature maximum. For points beyond this results were much less accurate unless a symmetry condition could be appropriately imposed on the solution. It was also demonstrated that for the case of temperature determination random errors in emission data and errors in an assumed concentration distribution were deamplified in the final result. In analogous studies for concentration, errors in input data were not reduced in the determined profile.

The simpler profiles of this study can be appropriately used to investigate the problems of simultaneously determining both temperature and concentration profiles from a set of spectral radiance measurements, a problem which is complicated by the fact that a set of spectral radiance measurements do not necessarily define a unique physical situation.

To infer anything about the spatial distribution of concentration and thus temperature requires additional information. The question becomes, how much information is needed and in what form should it be?

For the Fredholm integral equations of the first kind that describe the emission, no general statements about solution uniqueness can be made. One is forced to assume that the situation is defined well enough so as to allow only a narrow range of physical realistic solutions. To investigate what is necessary in order to give the simultaneous problem such definition, a series of numerical experiments were conducted. For all of these the physical length L of the hot gas region was assumed known. This is not an unreasonable assumption since for an internal application of spectral remote sensing L will be known exactly, and for an external case a reasonable approximation should not be difficult.

Simultaneous profile determination. The simplest possible application for simultaneous profile determination would be the case when both the temperature and concentration distributions can be exactly described by one parameter each. Figure 3 shows such a case for a pair of linear profiles where the single parameter is the slope. The initial approximation profile and those after the first and final iterations are shown. The final profiles (four iterations) agreed to within 0.5% with the exact. Thus the final and exact profiles are indistinguishable for graphical purposes. Actually, two parameters were used for each profile as would be expected for a linear curve, but the front boundary conditions were fixed through the use of

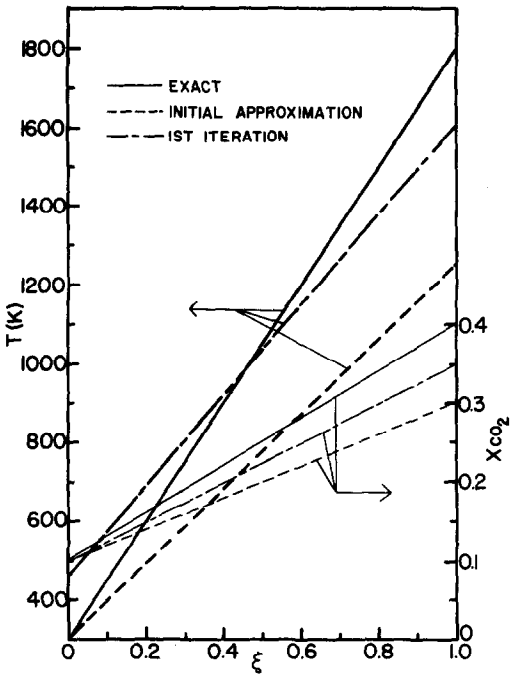

FIG. 3. Simultaneously determined single parameter temperature and concentration profiles, $L = 5.0$ cm.

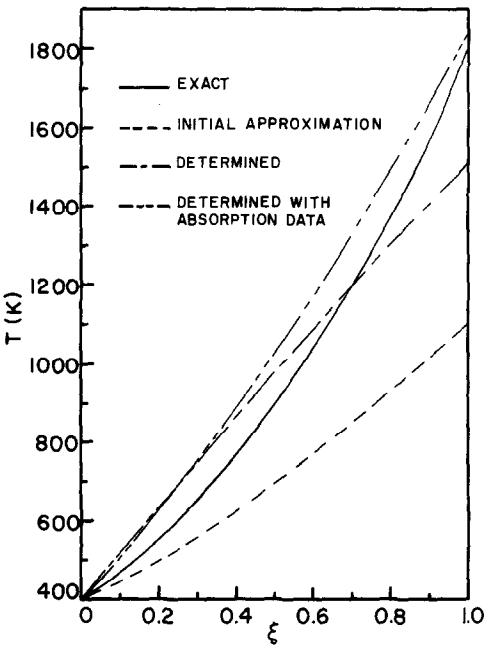

FIG. 4. Simultaneously determined two parameter temperature profile, $L = 5.0$ cm.

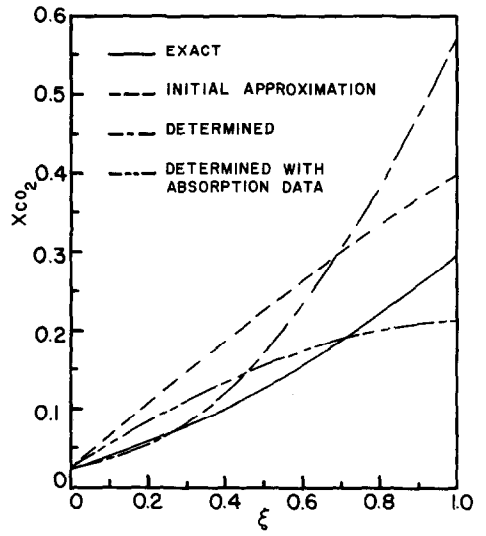

FIG. 5. Simultaneously determined two parameter concentration profile, $L = 5.0$ cm.

penalty functions so effectively there was only one degree of freedom per profile. The simulation was repeated for a number of initial guesses with the same result. This leads to the conclusion that for the limited case where the profiles are linear, simultaneous determination can be successful. These results were obtained using exact emission data; naturally the presence of data error would affect the determined profiles and this is discussed elsewhere [16].

A natural extension is to next consider profiles that can be exactly described by two parameters each. For example, a quadratic profile with the front boundary fixed would have two independent parameters. Figures 4 and 5 show determined temperature and concentration profiles respectively for such a system.

The profiles labeled determined were obtained using exact emission data. These results give average error values of 4.6% for intensity, 9.2% for temperature, and 38.5% for concentration ($0.1 \leqslant \xi \leqslant 1.0$). This indicates that although determined profile accuracy is not good, especially for concentration, the emission data is still fit to within a level that would be expected for experimental error. While this solution is not exact, it indicates that there is a range of acceptable solutions. This results from the non-uniqueness problems encountered as the unspecified concentration profile is given greater flexibility. For this case of exact emission data there may still be only one unique solution; however, it is clear that even with only two independent concentration parameters the ranges of solutions satisfying the data within experimental error may give highly erroneous concentration results.

One possibility to improve results in this situation is through the use of spectral absorption data. Such data would specify the optical thickness (X) given by

$$X(v) = \int_0^L k(v, T)\rho(s)\,ds. \tag{7}$$

Absorption data does not provide good spatial structure information, since the kernel in this case $k(v, T)$ is the absorption coefficient which does not depend directly on the space variable s but rather indirectly through its variation with temperature. This contrasts with the strong spatial variation of the exponential terms in the emission kernels. The data provide bounds for the total integrated concentration and thus should limit the range of acceptable solutions.

Absorption data can be introduced into the in-

version by simply adding to the index of performance a term of the form

$$\sum_{i=1}^{n} [X(v)_{\text{exact}} - X(v)_{\text{calc}}]^2.$$

At points far from the final solution, however, it is not clear what the relative weight of the absorption and emission terms in the index of performance should be. To overcome this, a procedure was adopted whereby only emission data is used at first. When a solution has been reached, the concentration profile is raised or lowered based on an average ratio of measured and calculated optical thicknesses. The emission based inversion procedure is then restarted with these new profiles. Once the optical thickness data points indicate different directions to move the concentration or are within 20% of the exact values, the absorption data is introduced directly into the inversion procedure to obtain a final solution.

Profiles obtained using absorption data are also indicated in Figs. 4 and 5. The average error values in this case were 2.2% for intensity, 10.5% for temperature, and 27.0% for concentration ($0.1 \leqslant \xi \leqslant 1.0$). As would be expected there is improvement in the concentration profile but the temperature remains about the same.

Still, even with this additional data and with little flexibility allowed in the solution profiles, there are clearly non-uniqueness problems when the concentration profile is left uncertain. In fact, it is likely that *a priori* knowledge will provide a better estimate of the concentration profile than can be had through simultaneous determination.

Single concentration determination. The previous results indicate that the accurate specification of a multiparameter concentration profile when the temperature distribution is also unknown will not, in general, be possible. There still remains, however, the possibility that if through *a priori* information the concentration can be characterized by a single parameter, this parameter plus the temperature profile can be accurately determined through inversion. The form of this parameter will, of course, depend on the physical situation and the source of *a priori* information, whether it be analytical predictions or experimental estimation.

One case where a single parameter characterization is definitely applicable is when the concentration distribution is uniform, the only unknown being the emitting species mole fraction. The final numerical experiment investigates single parameter determination in such a situation.

A search approach has been taken to determine the concentration parameter as opposed to locating it directly by the optimization routine. This is because of the conflicting search direction problems that can be encountered when both temperature and concentration are iterated. Specifically, a region around the expected solution is searched at each point the concentration is held constant and the best temperature fit determined. The solution parameter is then the one for which the determined temperature profile gave the lowest value of the index of performance (f).

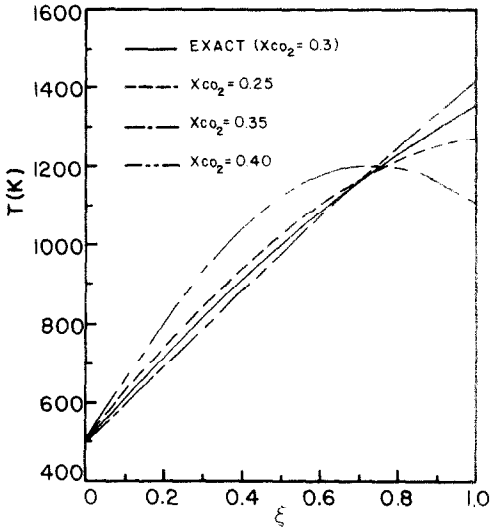

FIG. 6. Determined temperature profiles for various perturbed concentration levels. $L = 5.0$ cm.

Figure 6 shows a few determined temperature profiles for various parameter values. As would be expected, the further the concentration parameter from the exact value the more discrepancy in the determined temperature profiles. The front boundary temperature is fixed for these results. It is important to note whether the temperature profiles determined with erroneous concentration values have a larger value for the index of performance. For this case it was found that they did. This would make it appear that the determination of a single concentration parameter in addition to the temperature profile is possible. This simulation, however, does not account for additional uncertainties that may be present in an actual experiment.

EXPERIMENT STUDY

Apparatus

In order to provide a controllable gas path for studying the inversion problem a small laboratory furnace was constructed. The essential elements of the furnace are indicated in Fig. 7.

Basically the furnace consisted of an insulated stainless steel frame 45.7 × 43.2 × 43.2 cm. The insulation held in place a 55.9 cm silicon carbide tubular heater.* The heater is constructed in such a manner that heat is generated primarily in the middle 25.4 cm of the element. The heater was not suitable for gas containment, so another silicon carbide tube with a 2.54 cm I.D. was placed within the heater. This tube was outfitted with 19 chromel–alumel thermocouples imbedded at different depths within the walls. Measurements indicated negligible error between the thermocouple readings and the inside wall temperature of the tube. At one end the tube was fitted with a

*Carborundum Co., Refractories Division, Niagara Falls, New York, U.S.A.

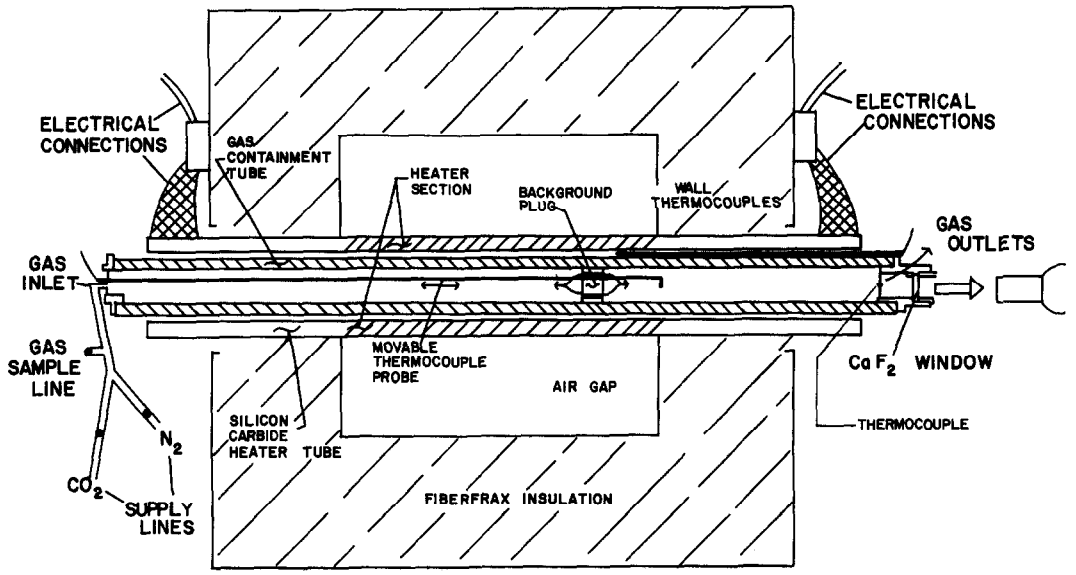

FIG. 7. Schematic diagram furnace assembly.

0.63 cm thick CaF_2 window with approximately 95% transmission in the spectral region of interest. The holder allowed for a 1.9 cm dia. exit for radiation.

As indicated in Fig. 7, a background plug was fitted into the gas containment tube. This plug served three functions: (1) since it was movable, its reposition varied the physical length of the test section thus changing the gas temperature profiles to be determined; (2) as a high emissivity radiation source, it simulates the effects that background walls might have in applying remote sensing to an internal situation; and (3) by limiting the length of the test section, it helps eliminate the possibility of the measuring instrument viewing the walls directly. Since the temperature of the plug is measured independently, it provides a known radiation source so that it presence does not change the essential nature of the problem, i.e. to determine the gas temperature profile. The plug had small holes to allow for gas flow and movement of the thermocouple probe. The remainder of the plug surface contained a series of cylindrical cavities drilled to increase the plug's emittance which was estimated to be 0.85.

The movable platinum vs platinum–10% rhodium thermocouple probe indicated in Fig. 7 was used primarily for gas temperature measurements over the first third of the gas path length. Beyond this point radial temperature gradients begin to significantly affect probe measurements so that comparison temperatures through the remainder of the gas path are more reliably based on predicted values and the thermocouple held in the gas stream by the window holder. The gas flow system allowed the gas stream to be sampled after the CO_2 and N_2 had mixed. The gas samples were then analyzed with a gas chromatograph to determine the CO_2 partial pressure.

The infrared spectral emission from the gas mixture was measured using a Barnes Spectralmaster Model 12-550 spectralradiometer, a remote and portable detector. The optics were set to give a narrow field of 2.5 mrad. At a distance of 2 m this gives a field of view of approximately 5 mm in diameter. The instrument was equipped with a two segment circular variable filter wheel that provides a continuous 1.6–5 μm scan. In the region around 4.3 μm the spectral resolution half bandwidth was 1.6 μm or 50 cm^{-1}. The instrument was calibrated using a blackbody source. The effects of bandwidth averaging were reduced by adjusting the measured values by the ratio of the emission at a particular frequency to that averaged over the bandwidth [16]. An approximate solution profile was used to generate this correction which was typically less than 10%.

Experimental results and discussion

Experimental conditions and data employed. The "furnace" was run for a number of different conditions; the results presented herein are for a path length of 25 cm with CO_2 partial pressures from 0.05 to 0.35 atm (total pressure 1 atm). Two temperature levels were used with peak values of approximately 1035 and 1350 K.

Six emission data points were used in the inversion routine. The points were spaced at approximately 0.04 μm intervals in the range from 4.28 to 4.6 μm. At higher CO_2 concentration levels the spectral data is shifted to the long wavelength region of this interval. The lower absorption coefficient values seen at longer wavelengths compensate for the increase in CO_2 concentration so that low optical thickness data (~ 0.5) is provided regardless of concentration.

For this experiment the spectral emission data can be approximately classified in three categories depending on optical thickness. For spectral data points with $X_v > 5$ [equation (7)] the gas is essentially opaque, and emission here serves to define gas temperatures at or near the front boundary. At intermediate optical thickness ($2 < X_v < 5$) the emission is still weighted

towards the front; however, layers further into the gas are now contributing so that these points provide information about the initial slope of the temperature profile. Finally, at points where $X_v < 2$ the emission is most heavily weighted at points well within the gas layer thereby providing gas temperature information away from the front boundary region. One data point taken from each of the three ranges is sufficient to define a three parameter temperature profile. To minimize the possible effects of data error, two points from each region were used.

In addition to emission data the inversion routine requires as input $I_v^-(L)$, the radiation intensity incident on the medium at the back face, equations (3) and (4). This can be done by viewing the plug with only nitrogen flowing in the test cell. This eliminates any gas emission or absorption. It was observed that the plug radiation corresponded very nearly to that of a black surface at approximately the plug temperature. This results because about 90% of the wall radiation incident on the plug comes from a 3 cm region adjacent to it. The wall temperatures here are very nearly equal to the plug, so essentially the plug and surrounding walls form an isothermal black cavity. Thus the measured values of $I_v^-(L)$ can also serve as a calibration check which can easily be taken within minutes of an experimental scan.

In addition to the thermocouple measurements made in the gas stream an analytical prediction of the gas temperature distribution was used to compare with inversion results.

The experimental situation was analyzed as a thermal entry length problem, one in which the tube wall temperature variation is known. The solution to this problem is well documented and the development of Kays [19] was adopted. Details of the solution are documented elsewhere [16]. Estimates were made of the effect of radiation on the temperature distribution. Results indicated that the effect was probably not sufficient to justify the complex analysis necessary to properly account for it.

The errors resulting from radiation interaction and the developing velocity profile will have their greatest effect at points near the outlet. To improve the reliability in this region, the inlet cold gas velocities were adjusted so that predicted profiles agreed with the downstream thermocouple reading. The indicated thermocouple temperature incorporates a radiation–conduction correction. Agreement was generally obtained with less than a 10% adjustment to the predicted outlet temperatures. It is felt that combining measured and predicted values in this manner provides the most reliable data with which to compare the inversion results.

Finally, the inversion results are compared against gas temperatures that represent an average of the radial temperature distribution over the instrument field of view which for the radiometer corresponds to about 25% of the tube diameter.

Determined temperature profiles. Figures 8 and 9 compare temperature profiles determined by the inversion procedure with that predicted and measured with thermocouples. A three parameter polynomial is used to represent this profile with $\eta = 1$, see equation (6). The determined temperature profiles for these figures were obtained using the measured concentration data. The earlier discussion of the kernel functions indicated that for profiles of this type where concentration level has been specified, spectral inversion should be able to determine the temperature accurately up to the peak. Since the peak temperature is located at the rear boundary, accurate determination of temperature throughout the gas path

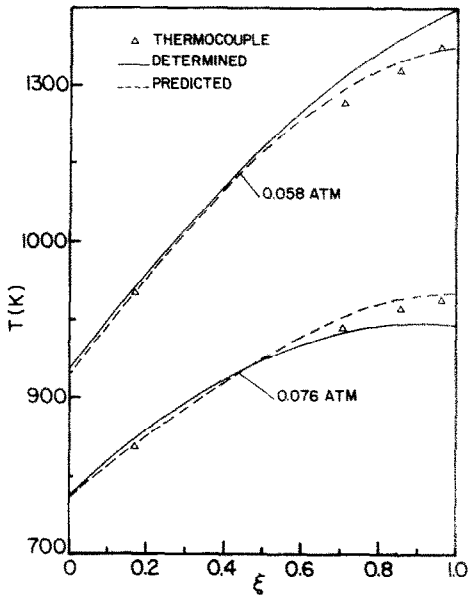

FIG. 8. Comparison of the determined temperature profile with that predicted and with thermocouple measurements, lowest CO_2 concentrations, $L = 25.0$ cm.

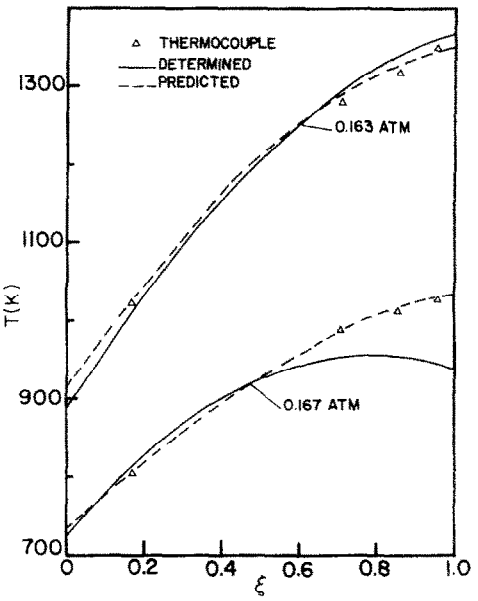

FIG. 9. Comparison of the determined temperature profiles with that predicted and with thermocouple measurements, medium CO_2 concentrations, $L = 25.0$ cm.

should be expected. In general, it can be seen that the experimental results verify the analytical trends, the average temperature error being only about 1.5%.

The increase in error seen towards the rear boundary can be partly explained by referring to Fig. 2 which shows that the kernel functions weighted more heavily toward the rear have less sharply defined maxima than those near the front; therefore, less discriminatory information about rear side conditions is contained in the emission data. This alone, however, would not account for a result as poor as that obtained for the low temperature case of Fig. 9, where the rear boundary temperature error is nearly 10%.

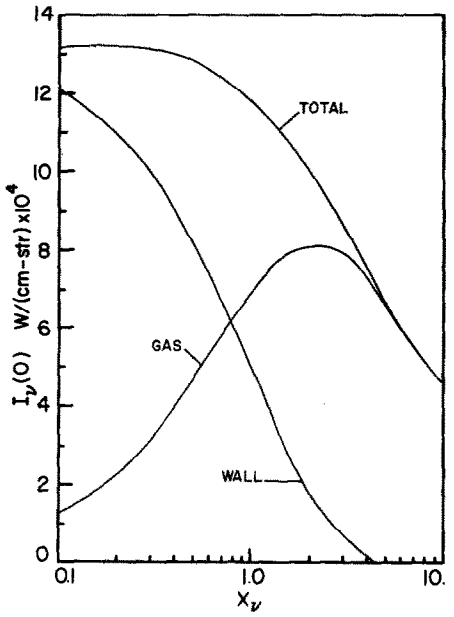

FIG. 10. Relative contribution to the total measured emission from the gas and background wall vs optical thickness.

For the experiment there are two additional factors not examined in the analytical studies which could cause such a result. First, there is the effect of the high temperature background wall (plug). This is shown in Fig. 10 which illustrates the variation with optical thickness* of the two components of the total emission, that from the wall and from the gas itself. It is seen that at low optical thickness (< 0.5) the measured emission comes predominantly from the wall. This means that the total emission at these points is more sensitive to how much the gas transmits the wall radiation than it is to the emission from the gas itself. This results in an increased range of acceptable solutions for the temperature in the rear boundary region, which will become more pronounced with an increase in emission data or absorption coefficient error. If it is known *a priori* that the gas and wall temperatures are equal at the rear boundary, then this effect can be largely overcome by requiring the inversion result satisfy this condition. Such a condition is likely to be the case whenever the gas is viewed perpendicular to the predominant flow direction. If the rear boundary temperature is fixed for the results of Figs. 8 and 9, agreement between measured and predicted temperatures for the region $0.5 \leqslant \xi \leqslant 1.0$ is within 1%.

The wall effect can also be minimized by avoiding the use of very low optical thickness data ($X_\nu < 0.4$) where the wall radiation is dominant. Unfortunately, this involves a compromise since it is these points for which the gas emission kernels are most heavily weighted in the rear region. It is important to note that this problem is peculiar to the case of a high temperature rear boundary. If the boundary is at a temperature significantly lower than the peak gas temperatures, then low optical thickness data can be used without this difficulty.

Despite the complicating effect of the high temperature boundary, these results and others obtained under similar conditions indicated that a parameter estimation spectral inversion procedure should be able to recover gas temperature profiles up to the peak value with an error based on absolute temperature of 3% or better. Of course, this is for the case of the emitting species distributed uniformly throughout the medium and when its concentration is known. The effects of uncertainties in the concentration level and the possibility of simultaneously determining that level will be examined in a later section.

Effects of location and number of data points. These results can be used to illustrate the effect of varying the number and spectral location of the data points. As discussed previously spectral data points were classified depending on whether they had low, intermediate, or high optical thickness values. It is of interest to study the effects on determined temperature profiles of deleting data in each of these ranges. This can be done by comparing three characteristic parameters of the determined temperature profiles: the front boundary temperature $T(0)$, the initial slope $dT/d\xi|_{\xi=0}$, and the maximum temperature which occurs at the rear boundary $T(1)$. Table 1 lists these parameters for five determined temperature profiles corresponding to the "high temperature" case of Fig. 9. Also listed are the optical thicknesses for each of the spectral data points used to determine the temperature profile. The results of the first line were obtained using the typical six data points with two in each optical thickness range. In each of the next three lines four data points are used where two points from each optical thickness region are deleted. The trends discussed earlier are in evidence here. Results obtained without the low optical thicknesses show the largest discrepancies at interior points as evidenced by the change in $T(1)$. Without the intermediate optical thicknesses the slope is affected while the boundary temperatures remain the same. Without the high optical thicknesses the front boundary temperature is affected which in turn affects the initial slope. The last

*It is plotted vs optical thickness rather than wavelength because the optical thickness for any particular wavelength depends on the CO_2 concentration. The approximate wavelength range in the figure is from 4.60 μm at $X_\nu = 0.1$ to 4.25 μm at $X_\nu = 10$.

Table 1. Effect of the number of data points and their optical thickness on determined temperature profile parameters

X	$T(0)$ [K]	$dT/d\xi\|_{\xi=0}$ [K]	$T(1)$ [K]
(1) 11.5, 8.7, 5.2 3.0, 1.6, 0.5	887.1	805.7	1368.9
(2) 11.5, 8.7, 5.2 3.0	890.9	742.4	1416.3
(3) 11.5, 8.7, 1.6 0.5	892.6	718.6	1386.1
(4) 5.2, 3.0, 1.6 0.5	914.2	695.3	1403.4
(5) 11.5, 5.2, 0.5	890.5	796.0	1362.9

line in the table gives results obtained with only three data points, one in each optical range. Comparison of this case with that using six points demonstrates that for the furnace profiles three data points is sufficient provided their spectral location is properly selected. In other situations the minimum number of data points needed may be more or less depending on the complexity of the temperature profile and the number of parameters needed to accurately describe it.

Effects of absorption coefficient data error. Another factor not present in the analytic studies is possible error in the band model used to predict the carbon dioxide emission. For this study such errors are most significant in the temperature range 600–1200 K. Particularly because there is considerable discrepancy at 600 K between the Malkus [8] data used for this study and the more recent data of Kunitomo and Osumi [20]. Also, the tabulated absorption data of Malkus as provided by Ludwig *et al.* [9] does not give any model parameters between 600 and 1200 K. For wavelengths on the P branch the absorption coefficient varies rapidly between these two temperatures. Thus the basis chosen for interpolating between the values will affect the calculated radiances especially for this experiment where much of the gas is at temperatures between 600 and 1200 K. Taking the absorption coefficient to vary with $T^{1.4}$ in this region gave consistently improved results and all the determined profiles of Figs. 8 and 9 used this interpolating scheme. A more complete discussion of the effects of absorption coefficient error may be found elsewhere [16]. It should be mentioned, however, that no particular significance should be attached to the exponent value 1/4. It merely provided a consistent and convenient means of interpolating band model parameters. A number of exponent values were tried: 0.25 gave consistently improved results, so it was used. No attempt to determine an optimum value was made.

Secondly, no attempt was made to make a parametric study of the effects of absorption coefficient error on inversion results. Such a study would likely be limited in its use since it would depend very much on the particular gas band employed for emission calculations and on the particular physical application. Rather, the more practical question of whether the presently available 4.3 μm CO_2 band model parameters are sufficiently accurate for use with an inversion procedure is of interest. The furnace experiment indicates that for the temperature range of 600–1200 K additional data would be helpful. However, accurate results can still be obtained in the presence of absorption coefficient error since there is no reason to expect that the adopted interpolating scheme yields exact values, especially considering the discrepancies indicated by the Kunitomo–Osumi [20] data.

Effect of concentration error. All the results given so far were obtained with the concentration level specified at the value measured by the gas chromatograph. It is of interest to examine the results further to determine what would be the effects when the concentration is not known exactly. Two aspects of the problem are important. First, what is the effect on the determined temperature profile of using an erroneous assumed concentration level? Second, how accurately can the concentration level be determined simultaneously along with the temperature distribution using the measured spectral emission data?

For the high temperature cases of Figs. 8 and 9, results were obtained using the identical emission data and initial approximations but with various perturbed concentration levels. As far as temperature determination is concerned, the trends encountered in similar analytical studies are in evidence here. Namely, error in concentration is de-amplified in the final temperature result. These results and others indicate, for example, that an error in concentration level on the order of ± 15% should give a temperature result which deviates from that obtained with the exact concentration by 2% or less. A graphical picture of the effect is provided in Fig. 11 which compares determined temperature profiles obtained with 0%, − 19.6%, and 19.6% error in assumed concentration level.

Figure 11 indicates the general level of error and trends in the determined temperature profile that can

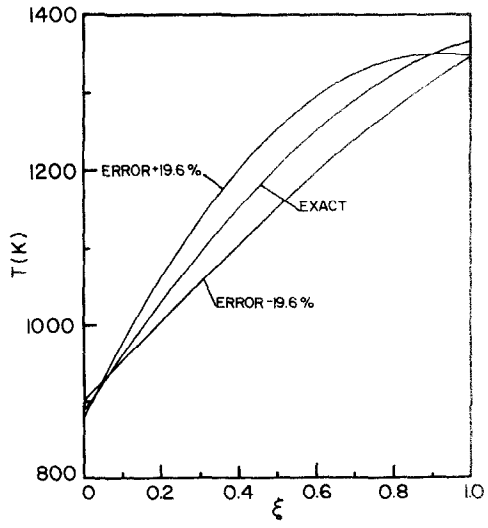

FIG. 11. Comparison of determined temperature profiles obtained with exact and perturbed concentration levels. p_{CO_2} (exact) = 0.163 atm, L = 25.0 cm.

be expected to result when erroneous concentration levels are used in the inversion procedure. Clearly, accurate results can still be obtained by spectral inversion for "furnace type profiles" in the presence of reasonable error in an assumed concentration level ($\pm 15\%$), a level which, for example, might have been estimated based on some *a priori* knowledge of the system.

In analytical experiments the question of determining both concentration and temperature from the emission measurements was examined. Results indicated that if the concentration could be characterized by a single parameter, then this parameter could be determined by a random search procedure. This was verified analytically on profiles very similar to those of the furnace experiment except without the background radiation source. Of course, for this situation where the profile is uniform, the concentration distribution is exactly described by a single parameter.

It is natural to apply the same procedure to the experimental data in an effort to determine the measured concentration. In the analytical experiments the concentration was inferred by determining the temperature profile for various concentration levels. The level for which the lowest value of the index of performance [equation (5)] is obtained is taken as the determined value. It is hoped that the graph of index of performance vs concentration will indicate a clear minimum as was the case for the analytical experiment.

Figure 12 plots the value of the index of performance f at a number of concentrations for three experimental cases. The actual points generated by a particular inversion run are indicated. It is immediately obvious from the figure that the sharp minima that allowed the concentration to be determined for the analytical study are not evident for the experimental data. This is

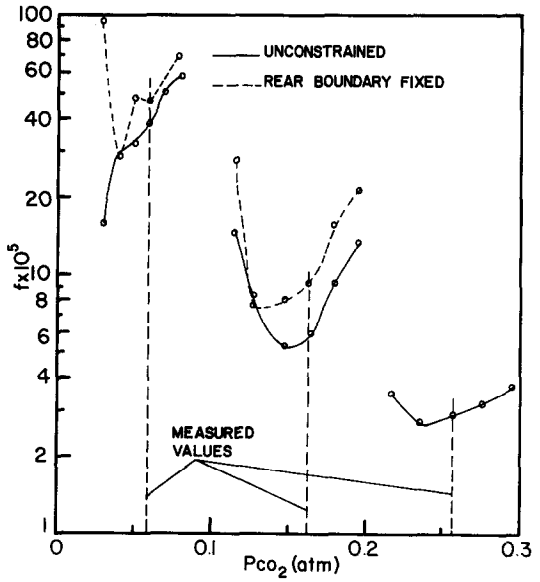

FIG. 12. Value of the index of performance for determined temperature profiles obtained using concentration levels perturbed about the measured values.

felt to result from two factors not present in the analytical studies. Random emission data error and probable errors in band model parameters will raise the f values and naturally tend to broaden the minima. Furthermore, there is the non-uniqueness introduced by the rear wall radiation. This effect is most pronounced at the low concentration where three of the six spectral data points have optical thicknesses low enough so that a significant contribution to emerging radiation comes from the wall. This explains the unexpected result obtained in this case, namely that no minimum is indicated within a reasonable range of the measured concentration. When the rear boundary temperature is fixed, which reduces the wall effect, there is a near order of magnitude increase in the value of f at the lowest concentration. With the rear boundary unspecified at this concentration ($p_{CO_2} = 0.028$ atm), the inversion procedure returned a physically unacceptable temperature profile, one for which the temperature first decreased and then increased along the path length. At low optical thickness data points the calculated emission from the gas itself for such a profile is well below that for the correct profile; however, the increased transmission of wall radiation due to the lower concentration and temperature compensates for this producing the same spectral distribution of emission as measured. At higher concentrations the wall effect diminishes, and results with and without the rear boundary fixed indicate the same trends. The difference is so small for the higher concentration case that the fixed boundary result is not shown.

The results of Fig. 12 and a similar study made for the lower temperature data indicate that in the presence of various sources of experimental error an emission based spectral inversion procedure will not accurately determine the concentration distribution when the temperature distribution is unknown. This is true even for the simple uniform distribution of this experiment.

If, however, the purpose of the search procedure is considered as an attempt to improve the determined temperature profile by systematically varying the concentration level, the results are not so negative. For example, if there were no independent measurements of temperature and concentration and the solution temperature profiles were taken to be those corresponding to minimum f value, then the temperature profile so determined would be within the accuracy of the predicted profile. This is true for all the data cases excluding the unconstrained lowest concentration case which is distorted by the wall effects. Indeed, for the highest concentration case the temperature profile corresponding to the minimum f gave a better fit to the predicted profile than that obtained using the measured concentration.

Thus despite the numerous sources of error for this experiment including uncertainties in emission calculations, spectral bandwidth averaging, wall radiation effects, and temperature gradients across the field of view, a spectral inversion procedure can yield de-

termined temperature profiles up to the peak with accuracy better than 5% with only general knowledge of the emitting species concentration. Of course, the more accurately the concentration can be specified, the better the determined temperature will be.

CONCLUSIONS

A number of conclusions about the usefulness and future applicability of spectral remote sensing can be made based on this work.

1. Parameter estimation in conjunction with a gradient based optimization routine was found to be a workable means of determining approximate solutions to the integral equation describing the spectral emitted intensity.

2. A low spectral resolution instrument such as the spectralradiometer can be used successfully for inversion work primarily because emission data error is de-amplified in the determined temperature profiles.

3. Comparison of measured and predicted emission for the experiment indicated some uncertainty in the 4.3 μm CO_2 band model parameters for the temperature range of 600–1200 K. Otherwise, it would appear that the Curtis–Godson approximation in conjunction with the property data used herein predicts emission from the 4.3 μm CO_2 band with sufficient accuracy for inversion work.

4. The experimental results indicate that for profiles of this study, agreement between measured and determined profiles on the order ot 3% can be expected. This was despite the uncertainty introduced by the rear wall radiation and the non-ideal effects of absorption coefficient error and radial temperature gradients. The presence of a strong rear boundary radiation source did prohibit, however, the accurate determination of concentration level in addition to the temperature distribution.

5. Both the analysis and experiment indicate that the information content in the spectral emission data alone is not sufficient to simultaneously determine both concentration and temperature profiles unless each of the profiles can be accurately described by a single parameter. They also indicate that a highly accurate specification of the concentration profile is not necessary for accurate temperature determination.

6. Any additional information such as a boundary temperature will improve results.

These experiments lead to the conclusion that even under experimental conditions spectral remote sensing if properly applied can be a useful and easily implemented high temperature gas diagnostic.

Acknowledgements—The authors wish to acknowledge the financial support of the National Science Foundation Heat Transfer Program under Grant No. GK 23373X and also for providing funds for the purchase of the continuous variable filter wheel under Grant No. ENG75-17097. Purdue Laboratory for Applied Industrial Control (PLAIC) provided support for one of the authors (P.J.H.) during the last year of his doctoral work. Computer facilities were made available by the Purdue University Computing Center.

REFERENCES

1. E. M. Sparrow and R. D. Cess, *Radiation Heat Transfer*, pp. 195–204. Brooks Cole, Belmont, CA (1970).
2. C. D. Rodgers, Retrieval of atmospheric temperature and composition from remote measurements of thermal radiation, *Rev. Geophys. Space Phys.* **14**, 609–624 (1976).
3. B. Krakov, Spectroscopic temperature measurement in inhomogeneous hot gases, *Appl. Optics* **6**, 201–208 (1966).
4. F. S. Simmons, C. B. Arnold and G. H. Lindquist, Calculation of radiation from hot H_2O and CO_2 viewed through a cool intervening atmosphere, *Appl. Optics* **9**, 2792–2794 (1970).
5. L. J. Muzio, E. S. Starkman and L. S. Caretto, The effect of temperature variations in the engine combustion chamber on formation and emission of nitrogen oxides, *S.A.E. Trans.* **80**, 652–662 (1971).
6. R. D. Cutting, The measurement of furnace temperature profiles by spectroscopic methods, Ph.D. Thesis, University of Newcastle, N.S.W., Australia (1973).
7. R. D. Cutting and I. McC. Stewart, Furnace temperature measurements by spectroscopic methods, *Appl. Optics* **14**, 2707–2711 (1975).
8. W. Malkmus, Infrared emissivity of carbon dioxide (4.3 μm band), *J. Opt. Soc. Am.* **53**, 951–961 (1963).
9. C. B. Ludwig, W. Malkmus, J. E. Reardon and J. A. L. Thomson, *Handbook of Infrared Radiation from Combustion Gases*, edited by R. Goulard and J. A. L. Thomson. NASA SP-3080, Washington, D.C. (1973).
10. A. R. Curtis, A statistical model for water-vapour absorption, *Quart. Jl R. Met. Soc.* **78**, 638–640 (1952).
11. W. L. Godson, The computation of infrared transmission by atmospheric water vapor, *J. Meteor.* **12**, 272–284 (1955).
12. M. T. Chahine, Determination of the temperature profile in an atmosphere from its outgoing radiance, *J. Opt. Soc. Am.* **58**, 1634–1637 (1968).
13. M. T. Chahine, A general relaxation method for inverse solution of the full radiative transfer equations, *J. Atmos. Sci.* **29**, 741–747 (1972).
14. R. Viskanta, P. J. Hommert and G. L. Groninger, Spectral remote sensing of temperature distribution in semitransparent solids heated by an external radiation source, *Appl. Optics* **14**, 428–437 (1975).
15. P. J. Hommert, R. Viskanta and R. E. Chupp, Application of spectral remote sensing of recovering temperature distribution in glass, *J. Am. Ceramics Soc.* **58**, 58–62 (1975).
16. P. J. Hommert, High temperature gas diagnostics by remote infrared spectral emission measurements, Ph.D. Thesis, Purdue University (1976).
17. R. Fletcher and M. J. D. Powell, A rapidly convergent descent method of minimization, *Comput. Jl* **3**, 163–168 (1963).
18. W. C. Davidon, Variable metric method for minimization, Argonne National Laboratory Report, ANL-5990, Argonne, IL (1959).
19. W. M. Kays, *Convective Heat and Mass Transfer*, Chapter 8. McGraw-Hill, New York (1966).
20. T. Kunimoto and M. Osumi, Narrow band model parameters for CO_2 4.3 μm band, *J. Quantve Spectres. Radiat. Transf.* **15**, 345–356 (1975).

DIAGNOSTIC DE GAZ A HAUTE TEMPERATURE PAR DES MESURES A DISTANCE

Résumé—On analyse l'utilité des mesures d'émission spectrale en déterminant les distributions rectilignes de température et/ou de concentration dans des systèmes gazeux à haute température. Un modèle analytique est construit qui relie l'intensité spectrale émise à la température locale et à la concentration d'espèces dans le gaz. L'établissement du modèle mathématique conduit à une série d'équations intégrales, une pour chaque fréquence de mesure. Les profils dans le gaz sont déterminés en inversant ces équations intégrales par utilisation d'une technique particulière. On conduit une étude expérimentale à des températures de gaz comprises entre 700 et 1350 K, pour une épaisseur de 25 cm dans un four électrique. Les gaz sont des mélanges CO^2/N^2 dont les fractions molaires varient en maintenant la pression totale égale à 1 atm. Les profils de température déterminés par inversion et les profiles mesurés indépendamment par thermocouple s'accordent avec une erreur moyenne inférieure à 3% (en utilisant les mesures de pression partielle de CO^2).

HOCHTEMPERATUR-GASUNTERSUCHUNGEN DURCH SPEKTRALE FEINABTASTUNG

Zusammenfassung—Die Nützlichkeit von spektralen Emissionsmessungen bei der Bestimmung von Temperatur—und/oder Konzentrationsverteilungen in Blickrichtung wird in Gasen hoher Temperatur untersucht. Es wird ein analytisches Modell angegeben, welches die emittierte spektrale Intensität mit der örtlichen Temperatur und Konzentration im Gas verbindet. Die mathematische Formulierung des Modells führt zu mehreren Integralgleichungen, eine für jede Frequenz, bei der Meßergebnisse vorliegen. Die Profile im Gas werden durch Umwandlung dieser Integralgleichungen unter Verwendung einer Parameter-Abschätzungs-Umkehrungstechnik bestimmt. Zusätzlich zu einer Anzahl von rechnerischen Untersuchungen wurde eine experimentelle Überprüfung in einem elektrisch beheizten Ofen an einem Gas bei Temperaturen zwischen 700 und 1350 K über einen Bereich von 25 cm durchgeführt. Das Gas bestand aus CO_2/N_2-Gemischen, deren Mol-Anteile bei einem konstanten Gesamtdruck von 1 atm variiert wurden. Die durch Umkehrung erhaltenen Temperaturprofile stimmten mit den Profilen, die aus Voraussagen und unabhängigen Thermoelement-Messungen erhalten wurden, mit einem mittleren Fehler von weniger als 3% überein (unter Verwendung von unabhängig gemessenen CO_2-Partialdrücken).

ДИАГНОСТИКА ВЫСОКОТЕМПЕРАТУРНЫХ ГАЗОВЫХ СИСТЕМ С ПОМОЩЬЮ СПЕКТРАЛЬНЫХ ДИСТАНЦИОННЫХ ИЗМЕРЕНИЙ

Аннотация — Исследуется возможность использования спектральных измерений излучения для расчёта находящихся на линии наблюдения полей температуры и концентрации в высокотемпературных газовых системах. Построена аналитическая модель, которая описывает зависимость между интенсивностью излучения, локальной температурой и концентрацией излучающих компонентов газа. Математическое описание модели приводит к ряду интегральных уравнений, каждое из которых предназначено для определенной частоты, при которой производились измерения. Профили температуры и концентрации определялись путем преобразования интегральных уравнений.